Compensation of the Low-Pass Filter Properties of the Current Measuring Internode in Potential-Clamped Myelinated Nerve Fibres

H. SCHUMANN, E. KOPPENHÖFER and H. WIESE

Institute of Physiology, University of Kiel, Olshausenstr. 40—60, D—2300 Kiel, Federal Republic of Germany

Abstract. The bandwidth of membrane current measurements in potential-clamped Ranvier nodes is limited by the low-pass filter properties of the internodes. If about 35% of the current measuring internode is grounded via an additional electrode, the bandwidth of this internode increases by a factor of about 40. Consequently, in potential clamp experiments the measured time course of the early ionic currents changes markedly, while the duration of the capacity current is shortened.

Key words: Myelinated nerve — Potential clamp — Current measuring internode

Introduction

In conventional potential clamp configurations for Ranvier nodes (Dodge and Frankenhaeuser 1958; Nonner 1969; Lonsky et al. 1972; Schumann 1980) the quantity of interest, the membrane current, equals U_E/Z_{DE}, where U_E is the output voltage of the clamp amplifier, and Z_{DE} is the impedance of the current measuring internode. The axoplasmic resistance of the internode and the radial capacity of the surrounding myelin sheath form a high-pass filter. The effect on current signals, however, is the same as that of a low-pass filter because the internode is part of a feedback loop, so it reduces the high frequency components of the current records (Nonner et al. 1978). A simple modification of the recording chamber (Koppenhöfer and Schumann 1981) enables a considerable increase in the corner frequency of the current measuring internode, which results in better time resolution of the chosen potential clamp system (see Fig. 2, Koppenhöfer and Schumann 1981). An analysis of the effects based on one-dimensional linear cable theory and some experimental results are presented in this report.

A preliminary report has been presented elsewhere (Schumann and Koppenhöfer 1981).

Cable Theory of the Internode

The axial current in a myelinated nerve fibre is assumed to flow along a cylinder of uniform cross section and to change only if current enters or leaves through the myelin sheath or the terminations of the internode.

Considering an infinitesimal segment of the internode, and following the one-dimensional linear cable theory (e.g. Jack et al. 1975), one obtains the partial differential equations of the transmyelin voltage $U(x,t)$

$$\partial U(x,t)/\partial x = -RI(x,t) \tag{1}$$

and

$$\partial^2 U(x,t)/\partial x^2 = RC_{my}\partial U(x,t)/\partial t\ , \tag{2}$$

where x is the distance along the internode, $I(x,t)$ is the intracellular axial current, R is the axoplasmic resistance, and C_{my} is the radial myelin capacity per unit length. The extracellular resistance as well as the conductance of the myelin sheath are assumed to be negligibly small.

In order to calculate the frequency response of an internode of finite length it is sufficient to treat only sinusoidal transmyelin voltages $U(x,t) = U(x)\exp(i\omega t)$. Then equation (2) may be written as

$$\partial^2 U(x)/\partial x^2 = \gamma^2 U(x) \tag{3}$$

with the propagation coefficient $\gamma = (i\omega RC_{my})^{1/2}$. Integrating the differential equation (3) over a finite length, L, and combining the result with equation (1) (Küpfmüller 1965) results in

$$U_L = U_0 \cosh(\gamma L) - I_0 Z \sinh(\gamma L) \tag{4}$$

$$I_L = -U_0 \sinh(\gamma L)/Z + I_0 \cosh(\gamma L)\ , \tag{5}$$

where U_0, I_0, U_L, I_L are the transmyelin voltages and the axial currents at each end of the regarded internode, and $Z = (R/i\omega C_{my})^{1/2}$ represents the characteristic impedance.

Conventional Potential Clamp

Fig. 1*a* shows the scheme of a conventional potential clamp recording chamber (Koppenhöfer and Schumann 1981). The nerve fibre is placed across 3 insulating gaps which separate the 4 fluid pools labelled A, B, C, and E. The node under investigation is located in pool A. Point D inside the node is kept at virtual ground potential, and the membrane current between point D and pool A is recorded as a voltage drop, U_E, across the internode between pools A and E by the specific potential clamp system. Because the following calculations are independent of

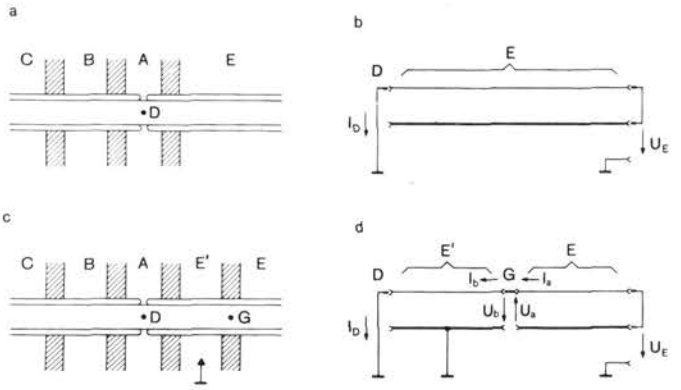

Fig. 1. a. Scheme of a nerve fibre in a conventional recording chamber. C, B, A and E: fluid pools separated by three insulating layers (shaded areas). D: point inside the node under investigation, kept on virtual ground by the specific electronic device. The neighbouring nodes are cut on both sides. **b.** Equivalent circuit in terms of distributed elements of the current measuring internode in pool E. The fibre is represented by a twin conductor (thin: axoplasm, thick: outside of the fibre, fluid in pool E). D: point inside the node, I_D: membrane current, U_E: output voltage of the clamp amplifier. **c.** Scheme of a nerve fibre in the modified recording chamber. The additional pool E′ is grounded. G: junction point of the two fibre segments between pool E′ and E. **d.** Equivalent circuit in terms of distributed elements of the current measuring internode in the modified configuration. U_a, U_b: transmyelin voltages at the junction point G. I_a, I_b: axial currents at G.

refinements of the specific clamp technique used, the external wiring of the recording chamber and the electrodes are not shown in Fig. 1.

In practice, the width of pool A is much smaller than the fibre length in pool E. Therefore, to simplify the following calculations, the distance between point D and side pool E was neglected. Fig. 1*b* shows the electrical equivalent circuit of the internode in pool E of the recording chamber in terms of distributed elements. The internode is represented by a four-terminal network containing a twin conductor (thin conductor: axoplasmic resistance R; thick conductor: fluid in pool E of negligible resistivity). The myelin capacity, C_{my}, is not shown here. The internode is short-circuited on the right end since it is cut close to the next node. The left end of the axoplasmic resistance is connected to point D and therefore kept at virtual ground potential. Assuming an ideal clamp system, the current I_D at point D equals the membrane current. The voltage across the myelin sheath between point D and the outside of the internode in pool E equals U_E.

If $Z_{DE} = U_E/I_D$ is defined to be the coupling impedance (Küpfmüller 1965) of the internode between pool E and point D (length $= L$), then application of the cable equation (4) with $I_0 = I_D$, $U_0 = U_E$ and $U_L = 0$ results in

$$Z_{DE} = Z \tanh(\gamma L) . \tag{6}$$

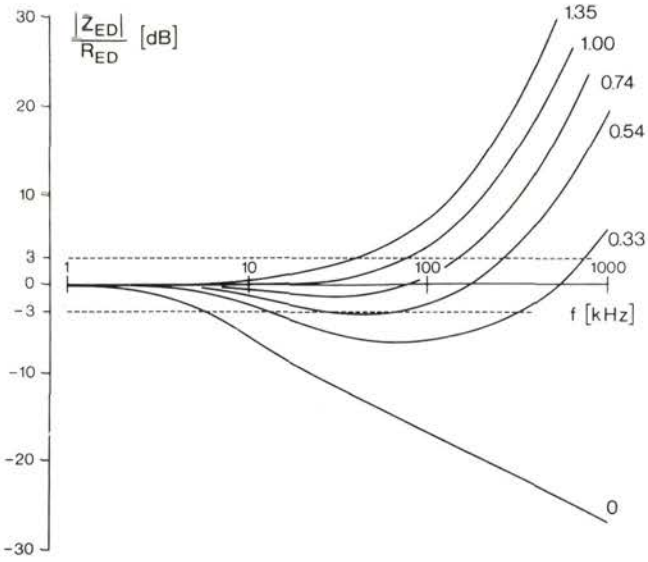

Fig. 2. Absolute value of the coupling impedance Z_{DE} of the current measuring internode related to the ohmic component R_{DE} as a function of the frequency f. The curves were calculated by equation (13) using an axoplasmic resistance $R = 14\ M\Omega/mm$, a myelin capacity $C_{my} = 1.3$ pF/mm and a length $L = l_{E'} + l_E = 2$ mm. The curves are labelled by the corresponding ratio $l_{E'}/l_E$.

The limiting case $\omega = 0$ yields the ohmic component of Z_{DE}, that is

$$R_{DE} = RL\ . \tag{7}$$

In conventional potential clamp configurations, equation (7) is used to calibrate the current records U_E (Dodge and Frankenhaeuser 1958). As a rule, the distinct reduction of the high frequency component of the effective frequency response (shown as Z_{DE}/R_{DE} in Fig. 2, curve 0) is neglected.

Modified Potential Clamp

The cut-off frequency of the internode (about 6 kHz, see Fig. 2, curve 0) can be shifted towards higher values by interposing a grounded pool E′ between pool A and E of a conventional recording chamber (Fig. 1*c*). As a result, the low-pass filter properties of the piece of internode remaining in pool E will be partially compensated by the grounded segment, which acts as a high-pass filter. The equivalent circuit shown in Fig. 1*d* was used to calculate the frequency response of the internode in the modified configuration. The two segments of the fibre are

located in two different pools (E′ and E). Therefore, the outsides of both segments (thick conductors) are insulated from each other while the distributed axoplasmic resistances (thin conductors) are coupled at the junction point G inside the fibre underneath the centre of the insulating gap between pools E′ and E. For G, then

$$I_a = I_b \,, \tag{8}$$

and

$$U_E = U_a + U_b \,. \tag{9}$$

Regarding the right segment of the internode one obtains from equation (6)

$$U_a/I_a = Z \tanh(\gamma l_E) \tag{10}$$

with l_E denoting the fibre length in pool E.

The application of the cable equations (4) and (5) to the left segment leads to

$$U_b/I_D = Z \sinh(\gamma l_{E'}) \tag{11}$$

$$U_b/I_b = Z \tanh(\gamma l_{E'}), \tag{12}$$

with $l_{E'}$ denoting the fibre length in pool E′. The equations (10) and (12) convert equation (8) to

$$U_a \,/\, \tanh(\gamma l_E) = U_b \,/\, \tanh(\gamma l_{E'})$$

and the introduction of equation (9) gives

$$U_E = U_b(1 + \tanh(\gamma l_E) \,/\, \tanh(\gamma l_{E'})) \,.$$

Replacing U_b in this equation by equation (11) and rearranging yields the coupling impedance $Z_{DE} = U_E/I_D$ of the modified configuration:

$$Z_{DE} = Z \cosh(\gamma l_{E'})\,(\tanh(\gamma l_{E'}) + \tanh(\gamma l_E)). \tag{13}$$

Setting $l_{E'} = 0$ and $l_E = L$, equation (13) converts to equation (6) which describes the conventional configuration. The ratio of the absolute value of Z_{DE} (determined from equation (13)) to R_{DE} is shown in Fig. 2. The increase in bandwidth obviously depends on the ratio $l_{E'}/l_E$ and the waviness of Z_{DE}/R_{DE} which can be tolerated. With $l_{E'}/l_E = 1$ (curve 1.00) and a maximal deviation of ± 3 dB the corner frequency is increased by about one decade as compared to the conventional configuration (curve 0). If the ratio $l_{E'}/l_E = 0.54$, the corresponding gain in bandwidth reaches a factor of about 40.

The diagram in Fig. 2 was calculated using the cable constants of a "standard" fibre of *Rana esculenta*, which are: $R = 14\ \mathrm{M\Omega/mm}$, and $C_{my} = 1.3$ pF/mm (Stämpfli and Hille 1976), and a length $L = l_{E'} + l_E = 2$ mm. Fig. 2 applies to every individual fibre if the frequency axis is scaled to

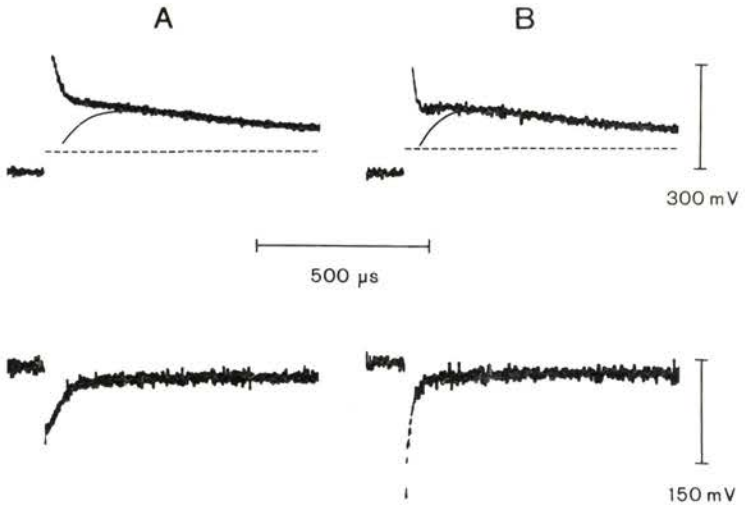

Fig. 3. Membrane current signals, U_E, elicited by test pulses of $V = 180$ mV (upper traces) and of $V = -50$ mV (lower traces). Corrections for the leakage current (dashed lines) and for the capacity current (continuous lines) were made as well for conventional measuring conditions, i.e. pool E′ connected to pool E (A), as for pool E′ connected to ground (B). Holding potential: −75 mV. Current signals are given in mV. The positive test pulses were preceded by a 50 ms negative prepulse of $V = -40$ mV. In the upper traces the peaks of the capacity currents are not shown. Fibre length in E′, $l_{E'} = 0.7$ mm, fibre length in E, $l_E = 0.8$ mm.

$$f' = f\, 43.1\, C_{my}/RL^2\,,$$

where R, C_{my} and L are the cable constants and the length of the specific internode given in MΩ/mm, pF/mm and mm, respectively.

Experimental Methods

Single myelinated nerve fibres (about 24 µm in diameter) were dissected from the sciatic nerve of the toad *Xenopus laevis* following the method of Sommer and Koppenhöfer (1982). The fibres were mounted in an appropriate perspex chamber for recording the membrane currents, corresponding to Fig. 1*c*. The node under investigation, located in compartment A, was superfused continuously by ordinary Ringer solution (in mmol/l: NaCl 112, KCl 2.5, CaCl 2.0, Tris (hydroxymethyl) — aminomethane HCl buffer 2.5; pH = 7.2 ± 0.1; $T = 8$°C). The adjacent internodes were cut close to the neighbouring nodes and placed in the side pools C, B, E′ and E, which were filled with artificial intracellular fluid (in mmol/l: KCl 108; NaCl 10; Tris-buffer 2.5; pH = 7.2 ± 0.1). Pool E′ could be connected either to ground or to pool E. Pools C, B, A and E were connected to a potential clamp system identical to that of Schumann (1980). The current signal (output voltage of the clamp amplifier, U_E) was filtered through a low-pass fourth order Bessel filter (−3 dB at 100 kHz). No compensation of the influence of the nodal series resistance was employed.

Table 1. Numerical solutions of the computer program for fitting the time course of Na current signals shown in Fig. 3. Time constants are given in ms, I'_{Na} in mV.

	I'_{Na}	τ_h	τ_m	a
pool E′ connected to pool E	165.2	861.2	57.6	3.4
pool E′ connected to ground	146.7	927.7	38.1	6.4

Results

Positive rectangular potential steps of V = 180 mV were applied and the resulting membrane currents were recorded (Fig. 3, upper traces). Corrections for both leakage current (dashed lines) and capacity current (continuous lines) were made graphically by means of negative pulses of $V = -50$ mV (Fig. 3, lower traces). Assuming that the remaining current is carried mainly by Na-ions, we fitted the resulting net currents to the expression

$$I_{Na} = I'_{Na}(1 - \exp(-t/\tau_m))^a \exp(-t/\tau_h)$$

(Frankenhaeuser 1960) by a nonlinear least square fit computer program (Schmücker 1979). This was done for records taken from one and the same fibre with pool E′ connected to E (conventional measuring conditions; Fig. 3*A*) and with pool E′ connected to ground (Fig. 3*B*). The data derived from the records shown in Fig. 3 are given in Table 1. Increasing the bandwidth of the current measuring internode by grounding pool E′ markedly affected the measured time course of Na activation: as a rule, the time constant τ_m diminished while the power of the m-term increased. Evidently, the inactivation process was influenced to a less extent: the time constant of the inactivation, τ_h, increased while I'_{Na}, decreased. Data derived from a second fibre matched with the data given in Table 1 satisfactorily well. Differences between the calculated and measured curves were too small to be demonstrated in a presentation like Fig. 3.

Discussion

The cut-off frequency of the current measuring internode in potential clamp studies on myelinated nerve fibres depends on the cable-like properties of the internode, and on the length. Therefore, in high resolution current measurements the internode is often cut as short as possible (Frankenhaeuser 1962; Nonner et al. 1978). Unfortunately, this diminishes the axoplasmic resistance and the amplitude of the current records; it enlarges the background noise in membrane noise measurements (Conti et al. 1976).

The improvement suggested in this report is obtained by intercalating an

additional pool (E′) between pool E and A of a conventional recording chamber. Since grounding pool E′ means a longer current measuring internode, there is no loss of amplitude of current signals. The calculation of the frequency response of the internode was simplified by using certain boundary conditions (mainly by assuming the inside of the Ranvier node to be a single point at ground potential).

The bandwidth of the internode in the modified configuration depends on the ratio of the fibre lengths in the pools E′ and E. The maximum gain in bandwidth, a factor of about 40, is considerably greater than predicted by the rough estimate in a preceeding paper (Koppenhöfer and Schumann 1981). Thus, the corner frequency of the internode in the modified configuration exceeds the bandwidth of present potential clamp systems (that is, the unity gain bandwidth of the loop gain, Nonner 1969) resulting in better time resolution of the current measurements in Ranvier nodes. In our opinion the data obtained by a broad-banded current measuring internode (Table 1, lower line) reflect changes of the nodal Na-permeability in a more authentic fashion than those derived from conventionally measured records. This holds for the capacity currents as well. Their peak value, as well as their duration, is obviously determined by the bandwidth of the current measuring internode; this has been shown both experimentally (Fig. 3, lower traces; Koppenhöfer and Schumann 1981; Wiese et al. 1982; Wiese and Koppenhöfer 1983) and theoretically (Wiese 1982; Wiese and Koppenhöfer 1983).

Acknowledgement. We thank Dr. A. Craig for his help with the English text.

References

Conti F., Hille B., Neumcke B., Nonner W., Stämpfli R. (1976): Measurements of the conductance of the sodium channel from current fluctuations at the node of Ranvier. J. Physiol. (London) **262,** 699—727

Dodge F. A., Frankenhaeuser B. (1958): Membrane currents in isolated frog nerve fibre under voltage clamp conditions. J. Physiol. (London) **143,** 76—90

Frankenhaeuser B. (1960): Quantitative description of sodium currents in myelinated nerve fibres of *Xenopus laevis*. J. Physiol. (London) **151,** 491—501

Frankenhaeuser B. (1962): Delayed currents in myelinated nerve fibres of *Xenopus laevis* investigated with voltage clamp technique. J. Physiol. (London) **160,** 40—45

Jack J. J. B., Noble D., Tsien R. W. (1975): Electric Current Flow in Excitable Cells. Clarendon Press, Oxford, pp. 25—60

Koppenhöfer E., Schumann H. (1981): A method for increasing the frequency response of voltage clamped myelinated nerve fibres. Pflügers Arch. **390,** 288—289

Küpfmüller K. (1965): Einführung in die theoretische Elektrotechnik. Springer, Berlin, pp. 377—420

Lonsky A. V., Ilyin V., Malov A. M. (1972): Improved device for potential recording from the membrane of nodes of Ranvier. Sechenov Physiol. J. USSR **58,** 136—138

Nonner W. (1969): A new voltage clamp method for Ranvier nodes. Pflügers Arch. **309,** 176—192

Nonner W., Rojas E., Stämpfli R. (1978): Asymmetrical displacement currents in the membrane of frog myelinated nerve: early time course and effects of membrane potential. Pflügers Arch. **375,** 75—85

Schmücker P. (1979): Computerunterstützte Datenanalyseverfahren zu biophysikalischen Membranmodellen. Diplomarbeit, Universität Kiel

Schumann H. (1980): Kompensation der elektrischen Auswirkungen des perinodalen Zugriffswiderstandes bei Ionenstrommessungen am Ranvierschen Schnürring. Thesis, Universität Kiel

Schumann H., Koppenhöfer E. (1981): Compensation of the low-pass properties of the current measuring internode in voltage clamped myelinated nerve fibres. Biophys. Structure Mechanism **7,** 317

Sommer R.-G., Koppenhöfer E. (1982): Präparation und Beurteilung isolierter Nervenfasern — Fortschritte in der Membranforschung. Microskopion (Wild Heerbrugg) N° 40, 4—6

Stämpfli R., Hille B. (1976): Electrophysiology of the peripheral myelinated nerve. In: Frog Neurobiology (Eds. R. Llinás, W. Precht) pp. 3—32 Springer, New York

Wiese H. (1982): The influence of different parameters on the capacity current in potential clamped Ranvier nodes. Pflügers Arch. **392,** R34

Wiese H., Koppenhöfer E., Stüning D. (1982): Capacity currents in potential clamped Ranvier nodes. Pflügers Arch. **394,** R47

Wiese H., Koppenhöfer E. (1983): On the capacity current in myelinated nerve fibres. Gen. Physiol. Biophys. **2,** 297—312

Received January 31, 1983 / Accepted March 1, 1983